Journal of Building Engineering 46 (2022) 103657

Contents lists available at ScienceDirect

Journal of Building Engineering

journal homepage: www.elsevier.com/locate/jobe

Activity concentration of the uranium and thorium series and exhalation rates of ^{222}Rn and ^{220}Rn in building material derived from niobium residues

Paulo Sergio Cardoso da Silva [a,*], Thammiris Mohamad El Hajj [b,**], G.A.S. A. Dantas [c], Homero Delboni Jr [c], Mauro Gandolla [d]

[a] Instituto de Pesquisas Energéticas e Nucleares (IPEN / CNEN - SP), Av. Professor Lineu Prestes 2242, 05508-000, São Paulo, SP, Brazil
[b] Universidade Federal de Alfenas (UNIFAL-MG), Rodovia José Aurélio Vilela, 11999, 37715-400, Poços de Caldas, MG, Brazil
[c] Universidade de São Paulo (USP), Rua Professor Melo Moraes, 2373, 05508-900, São Paulo, SP, Brazil
[d] ECONS SA, Via Stazione 19, 6934, Bioggio, Ticino, Switzerland

ARTICLE INFO

Keywords:
Radiological assessment
Sustainability
Niobium mining waste
Exhalation rate
Aggregates
NORM

ABSTRACT

One way to better manage mining waste may be to reduce its quantity by reusing it. Using waste as construction material in the case of the niobium industry might be feasible, even though it carries radioactive elements. This study evaluates the radiological impact of using niobium waste as a building material. Samples of niobium waste with and without granulometric classification were tested. Moreover, concrete proof bodies, concrete plates, and common commercially available aggregates and cement were radiologically assessed for comparison purposes. The main conclusion is that niobium waste might be both physically and radiologically suitable to manufacture concrete respecting boundary conditions.

1. Introduction

Many minerals and ores are classified as Naturally Occurring Radioactive Materials NORM). Therefore, under unfavorable conditions, may pose radiation risk to individuals. Mining and other industrial activities that involve minerals and raw material such as phosphate [1], monazitic sand [2], bauxite [3], coal [4], and metals mining [5,6] have the potential to increase the effective dose received by workers as well as by members of the public from natural sources: soil, water, and air [7]. During the extraction of minerals from the Earth's crust and their physical or chemical processing, the radionuclides may become unevenly distributed between the various materials arising from crushing, grinding, mineral and chemical extraction processes [8].

Mining involves the actual extraction of ores and inherently associated waste material, the latter consisting of non-mineralized or even low-grade rocks [9]. Mined ores are subsequentially processed for separating valuable minerals from gangue, thus resulting in concentrates and tailings. Mining waste and mineral processing tailings require appropriate disposal and management due to the possible associated high environmental impact. These materials may also contain trace elements, including radionuclides.

Recently, in Brazil, we have witnessed the catastrophic consequences of poor tailings management that lead to the Mariana and Brumadinho dam disasters. One way to better manage mining waste may be to reduce its quantity by reusing it. This concept has played a crucial role in maximizing resource utilization aiming to reduce environmental impacts [10]. A key focus on attaining

* Corresponding author.
** Corresponding author.
E-mail address: pscsilva@ipen.br (P.S. Cardoso da Silva).

https://doi.org/10.1016/j.jobe.2021.103657
Received 2 August 2021; Received in revised form 8 November 2021; Accepted 11 November 2021
Available online 14 November 2021

sustainability in mining activities is effective waste removal within the production processes.

One of the main potential applications of solid mining wastes and dry slurry is construction material [11–15] mainly in the concrete industry [16,17]. Nevertheless, the use of mining waste as recycled materials demands safety requirements for its application due to the possible presence of toxic compounds such as asbestos-like minerals, heavy metals, and exposure from naturally occurring radionuclides [18]. Regarding the radioactive aspects, in Brazil, the installations that process only materials with a specific activity $\leq$1 Bq g^{-1} and do not subject workers to dose increase above 1 mSv y^{-1} are exempt from radiological control. However, there is no legislation limiting the use of solid mining waste.

This study evaluates potential exposure to radiation caused by using niobium waste in concrete plates and proof bodies. The activity concentrations of ^{238}U, ^{226}Ra, ^{210}Pb, ^{232}Th, ^{228}Th, ^{228}Ra, and ^{40}K were determined in concrete made with niobium waste. The results were compared to commercial aggregate and cement. Exhalation rates for ^{222}Rn and ^{220}Rn were determined for concrete plates and proof bodies made with commercial concrete without the niobium waste (0%), with a mixture of 50% of niobium waste and commercial aggregate, and with 100% of niobium waste.

2. Theory

Radiation exposure to the human body occurs mainly from external gamma rays of ^{238}U, ^{232} Th day series, as well as of ^{40}K. On the other hand, internal exposure occurs by inhalation of radon exhaled from soil and rock in the ground and building materials, and from its progeny of short half lives. There are three radon isotopes: ^{222}Rn (radon), ^{220}Rn (thoron), and ^{219}Rn (actinon), whose half-lives are 3.82 d, 55.6 s and less than 4 s, respectively. Due to the noticeably short half-lives, thoron and actinon contribution to the total dose received by a human body, even in closed environments, was generally not considered. Nevertheless, recent studies have shown that the thoron contribution for the effective dose may not be negligible [19–21].

Depending on the local ground, the building construction and the buildings materials used, ^{222}Rn activity concentration in buildings may increase above the reference values of 300 Bq m^{-3}, established by the International Agency of Atomic Energy (IAEA). It may occur in houses built from materials which show radiation levels above normal background [22], for example, when using recycled materials from the mining process. Besides, a number of variables may also influence radon exhalation in dwellings, such as outdoor and indoor temperature, air pressure, humidity fluctuations, porosity, pore distribution and pore type, type of surface treatment at the building site and type of the coating material applied [23]. Radiological assessment is thus necessary in mining waste used as building material, particularly ^{238}U and ^{232}Th activity concentration, as well as respective decay products and exhalation rates.

3. Experimental

3.1. Sample description

The samples analyzed in this study were taken from a niobium mine, identified as Industry A in this article. The samples were taken from a stream of material called non-processed waste. This material is separated from the ore in a conveyor belt before entry in the processing plant. The separation is done using a using a magnetic field, the non-magnetic flow is then called non-processed waste. In this study, we refer to this material as niobium waste. The samples were taken and were then sieved to separate the granulometric fractions normally used in the aggregate industry.

The samples were classified as sand (grain size lower than 2.0 mm), crushed stone (grain size smaller than 6.7 mm), gravel 0 (grain size smaller than 13.2 mm) and gravel 1 (grain size smaller than 26.5 mm). A sample of niobium waste without sizing was also analyzed. All these samples will be named here as aggregates. In each case, an amount of 10 kg of the material was received from Industry A. The material was homogenized, and an aliquot of 300 g was taken for analysis. For comparison, two commercial aggregates of the same granulometry and one sample of cement commercialized in the regular market were selected, acquired and analyzed. For these commercialized samples, no information was available about their geological origin. Twelve concrete plates and nine proof bodies of approximately 3.5 kg were manufactured with the proportion of 0%, 50%, and 100% of three batches of waste material by the Federal University of Goias (UFG) to evaluate the exhalation rates. UFG was involved in proving the physical suitability of the concrete samples following the Brazilian Association of Technical Standards (ABNT). After they finished their research, they shipped the samples to the Institute of Nuclear and Energy Research (IPEN) for radiological characterization. Gamma spectrometry, neutron activation analysis and radon/thoron measurements were carried out on all above listed samples, as described in the following sections.

3.2. Gamma spectrometry

Gamma spectrometry was used to measure the activity concentrations of ^{226}Ra, ^{210}Pb, ^{228}Th, ^{228}Ra, and ^{40}K in samples of cement, waste, sand, crushed stone, gravel 0 and gravel 1, and powdered proof bodies. The proof bodies were cut, crushed, and ground for this analysis. For these measurements, to avoid radon loss, samples weighing from 50 to 60 g were sealed in polypropylene 50 mL plastic cans for at least 30 days before the measurement to ensure equilibrium between ^{226}Ra and its short half-life progeny [24]. Activity concentrations were determined using an HPGe detector, model GX 2020, from Canberra Industries with 1.50 keV and 2.5 keV of resolution for the 122 keV and 1332 keV of ^{57}Co and ^{60}Co, respectively. The reference materials RGU, RGTh, and RGK, from IAEA, were used for efficiency calibration, while calibrated sources of ^{60}Co, ^{137}Cs, ^{152}Eu and ^{241}Am were used for energy calibration. To determine ^{226}Ra activity concentration, the mean value of three decay transitions of its progeny, 295 keV and 352 keV of ^{214}Pb and 609 keV of ^{214}Bi, were considered. The activity concentration of ^{210}Pb was determined by measuring its low energy peak (46.5 keV). Self-absorption correction was applied to attenuate of the low energy gamma-ray, highly dependent upon sample composition [25].

The Lower Limit of Detection (LLD) for this measurement configuration was 1.8 Bq kg^{-1}. For ^{228}Ra activity concentration determination, the mean values of the decay transition in 338 keV and 911 keV of ^{228}Ac were used (LLD of 3.6 Bq kg^{-1}). The mean values of the decay transition in 238 keV of ^{212}Pb and 727 keV of ^{212}Bi were used to determine ^{228}Th (LLD of 4.0 Bq kg^{-1}). The decay transition in 1460 keV energy directly measure ^{40}K activity concentration (LLD of 17 Bq kg^{-1}).

3.3. Neutron activation analysis

The activity concentrations of ^{238}U and ^{232}Th were measured by neutron activation analysis [26]. Neutron activation consists in a nuclear reaction in which a nucleus undergoes a neutron capture process, resulting in a new nuclide that will decay according to its own nuclear properties. The neutron activation of ^{238}U and ^{232}Th forms ^{239}Np and ^{233}Pa, after beta decay, with half lives of 2.35 d and 27 d, respectively. The measurement of the gamma ray transitions in 228 and 277 keV gives the ^{238}U concentration, while the gamma ray transition in 312 keV, gives the ^{232}Th concentration when comparing the activity measured in the sample with that measured in a reference material.

Approximately 150 mg of each sample was weighed and packed in plastic polyethylene bags and further pre-cleaned with a diluted nitric acid solution. Samples were irradiated together with two reference materials (RM), USGS STM-2 and NIST SRM 1646a, and a standard solution of the elements of interest was pipetted into a paper filter. For each sample, the concentration was calculated in relation to each reference material, and the final report of the results is the mean value related to each RM. Samples and RMs were irradiated for 8 h in the IEA-R1 research reactor at IPEN under a thermal neutron flux of 10^{12} cm^{-2} s^{-1}. Decay periods of 7 and 15 days were adopted respectively for uranium and thorium for induced activity measurements.

The counting time of 1 h was used to determine the activity concentration of each sample and RM. Gamma spectrometry was performed by using an EG&G Ortec HP-Ge Gamma Spectrometer detector (AMETEK Inc., USA) and associated electronics, with a resolution of 0.88 and 1.90 keV for ^{57}Co (122 keV) and ^{60}Co (1332 keV), respectively. In these conditions, the Minimum Detectable Activity (MDA) is 12.6 Bq kq^{-1} for ^{238}U and 1.5 Bq kq^{-1} for ^{232}Th. The data analysis was carried out using in-house gamma-ray software (the VISPECT program) to identify the gamma-ray peaks. The methodology evaluation was performed by cross-checking the reference materials and synthetic standards.

3.4. Radon and thoron measurement

For ^{222}Rn and ^{220}Rn measurements, a RAD7 (manufactured by Durridge Co., Inc.) detector was used, which consists of an alpha particle detector that converts alpha radiation into an electric signal, distinguishing the energy of each particle, which allows the identification of the isotopes (^{218}Po and ^{214}Po from ^{222}Rn and ^{216}Po from ^{220}Rn) produced by radon decay. RAD7 calibration was carried out at Durridge's indoor facility, using a radon chamber with a radium (^{226}Ra) source to provide a known ^{222}Rn flow. According to the RAD7 User Manual, the reproducibility is generally better than 2%, and calibration accuracy is in the range of 5% [1, 27].

For ^{222}Rn, the exhalation rate was calculated following the formula given by Eq. (1) [28].

$$E_0 = \frac{C\lambda_{eff}V}{1 - e^{-\lambda_{eff}t}} \tag{1}$$

Where C is the equilibrium concentration, in Bq m^{-3}; λ_{eff} is the effective decay constant (s^{-1}), valid if leakage of radon and thoron

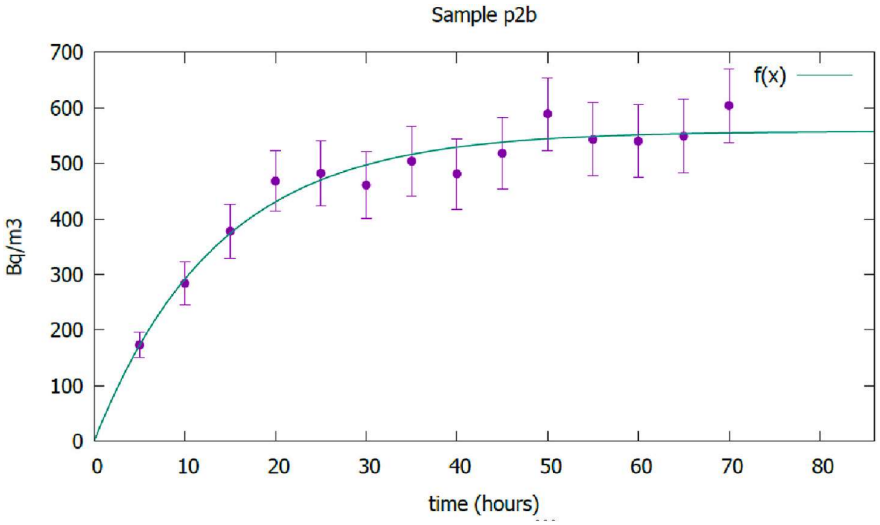

Fig. 1. Example of non-linear exponential regression for ^{222}Rn. Point and whiskers are the measured values, and the line is the theoretical fit obtained using the De Martino et al. [28] approach.

out of the sample container is possible and if the activity concentration in the container air is low compared to the activity concentration in the pore air of the sample; V is the effective volume of the chamber containing the sample plus tubes and the measurement chamber of the radon monitor, in m^{-3}; and t is time (s). The approach used in this study followed De Martino et al. [29], applying a non-linear curve fit to experimental data C versus t, in the form $y = a\ (1 - e^{-bx})$, where $a = E_0/\lambda_{eff}$ x V and $b = \lambda_{eff}$, where E_0 is the exhalation rate, λ_{eff} is the effective decay constant and V, the effective volume. Fig. 1 shows an example of the nonlinear exponential regression fit used for the exhalation rate determination from activity concentration values as a function of time.

All radon and thoron measurements were carried out in a closed system to avoid dilution. However, thoron measurements are probably underestimated because of the short half-life. For aggregate samples exhalation rate determinations (Fig. 2), an aliquot of approximately 300 g of each sample was placed inside an acrylic cylinder with 5 cm diameter and 200 cm length. In case of the plates (Fig. 3), each one was covered with a 2 mm thick plastic film and sealed at the edges with adhesive tape to prevent Rn from escaping. The proof bodies (Fig. 4) were put inside a plastic can, also sealed with adhesive tape.

In order to estimate if any radon loss could result from the measurement arrangement used in this study, the reproducibility of the results was tested by measuring a set of same samples in two independent team's lab, one located in Brazil and the other in Switzerland, using the same conditions, the same type of radon monitor and plastic membranes of the same density and composition [30]. Results, not presented here, showed no significant difference.

4. Results and discussion

Table 1 shows the activity concentrations measured in the aggregate samples of niobium waste from Industry A. From each type of aggregate, one aliquot of the homogenized sample was taken: waste with no sizing applied (IA-W), sand (IA-S), crushed stone (IA-CS), gravel 0 (IA-G0), and gravel 1 (IA-G1). For comparison, the same type of aggregates, with identical size grain particles, was obtained from the local market and were named here as commercial 1 (C1) and commercial 2 (C2), representing their trademarks. Also, one commercial cement sample, acquired in the local market (cement), was analyzed.

Table 1 shows that the activity concentration of the radionuclides from the U series (^{238}U, ^{226}Ra, and ^{210}Pb) were lower than 125 Bq kg^{-1}, which is considered relatively low compared to the radionuclide of the Th series (^{232}Th, ^{228}Th, and ^{228}Ra). The radionuclides ^{238}U and ^{226}Ra activity concentrations did not show significant differences according to the origin, i.e., from the niobium waste or the local market. Only ^{210}Pb presented higher concentrations in gravel 0 and 1 in the niobium waste aggregate samples. The high ^{210}Pb activity concentration may occur due to the higher half-live of U daughters and its chemical behavior during weathering processes with ^{210}Pb being accumulated in oxidized formations [31].

The marketed cement sample presented the same range of concentration for the nuclides of the U and Th series and ^{40}K. Eštoková and Palaščáková [32] reported a compilation of ^{226}Ra, ^{232}Th, and ^{40}K activity concentrations in types of cements found in 16 different countries whose values vary from 12 to 92 Bq kg^{-1}; 14–59 Bq kg^{-1} and 93–1133 Bq kg^{-1}, respectively. Özdis et al. [33] compiled information given in 19 articles from 14 countries for the activity concentrations of the same radionuclides, finding values in the range of 20–119 Bq kg^{-1} for ^{226}Ra, from 9 to 59 Bq kg^{-1} for ^{232}Th and from 51 to 2493 Bq kg^{-1} to ^{40}K. In Brazilian cement the concentration rage varies for 50–204 Bq kg^{-1} for ^{226}Ra, from 20 to 192 Bq kg^{-1} for ^{232}Th and from 160 to 550 Bq kg^{-1} to ^{40}K [34]. The activity concentration of these radionuclides in the cement raw materials depends on geological and geographical conditions, and geochemical characteristics of those materials [35]. However, the activity concentrations measured in the marketed sample in this study are in good

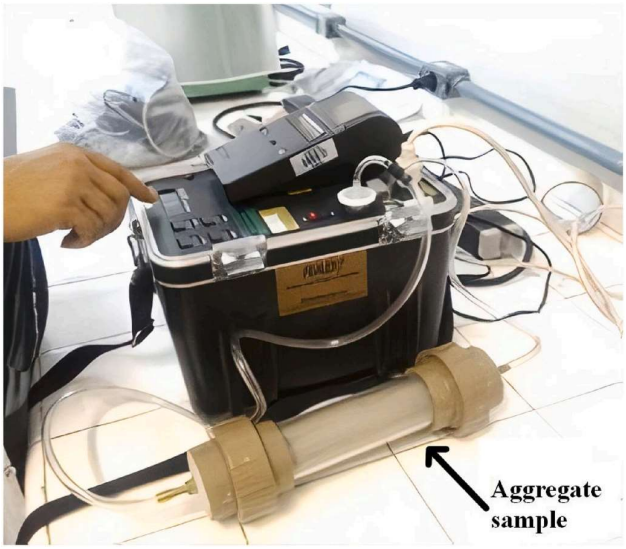

Fig. 2. Experimental apparatus for radon exhalation rate measurement in aggregate samples.

Fig. 3. Experimental apparatus for radon exhalation rate measurement in plate samples.

Fig. 4. Experimental apparatus for radon exhalation rate measurement in proof bodies samples.

agreement with those reported for various locations in different countries and the one reported for other Brazilian samples.

The activity concentration of Th series nuclides in the concrete made with Industry A waste, on the other hand, presented much higher values. It can also be observed for sand, crushed stones, gravel 0 and gravel 1. This amount of thorium is related to the mineralogy of the mined material composed of phyllite, carbonatites, and amphibolites [36]. It is also associated with high rare earth element concentration [37]. The values presented in Table 1 also reveal that the non-classified waste presented an activity concentration higher than the aggregates. These differences may result from the fact that the aggregates were wet sieved leaving the excess of Th nuclides daughters in the wash water, or due to an unexpected non-homogeneity between the fraction used in the non-classified sample and the sieved samples used to obtain the aggregates. Future studies must include the analysis of the waste water from the washing process and the remaining waste of the classified aggregates in order to clarify the differences observed here that must also be taken into consideration for radiological protection purposes.

Figs. 5–7 show the distribution of the radionuclides from the U and Th series and ^{40}K in the powdered proof bodies manufactured with different concentrations of the niobium waste (aggregate), 0% (no addition of niobium waste aggregate material), 50% and 100%.

Fig. 5 shows relatively small variation for both ^{238}U and ^{226}Ra. ^{210}Pb is the only nuclide that presents a wide range varying from 24 to 190 Bq kg^{-1}. Accordingly, the variation for ^{238}U was within the 20–55 Bq kg^{-1} range, while ^{226}Ra values the range were within an even narrower range ie. 40–60 Bq kg^{-1} apart from the above mentioned PB1-100% samples, which showed 110 Bq kg^{-1}. The activity concentration of ^{238}U was below the detection limit in samples PB1 and PB2 made with 100% of the niobium waste aggregate. The

Table 1
Activity concentrations measured in the cement, waste (W), sand (S), crushed stone (CS), gravel 0 (G0) and gravel 1 (G1) samples from Industry A, and aggregates commercialized in the region (C1 and C2 representing two different aggregates trademarks).

Activity concentrations (Bq kg^{-1})														
Sample	^{238}U		^{226}Ra		^{210}Pb		^{232}Th		^{228}Th		^{228}Ra		^{40}K	
Cement obtained in the regular market														
Cement	19	±2	23	±1	7	±11	21	±1	28	±5	24	±4	247	±5
Aggregates of niobium waste samples from Industry A (IA)														
IA-W	ND*		76	±3	ND		4839	±299	2269	±18	2162	±13	182	±10
IA-S	16	±9	65	±2	66	±16	1050	±54	854	±8	800	±7	853	±8
IA-CS	71	±11	57	±3	645	±14	1651	±102	820	±11	725	±9	947	±11
IA-G0	89	±6	42	±2	789	±13	1529	±86	902	±15	844	±6	869	±9
IA-G1	81	±6	57	±3	ND		1249	±70	738	±9	689	±6	834	±10
Commercialized aggregate samples, named "G" and "PB" in this study, obtained in the regular market														
C1–S	121	±8	113	±2	359	±5	122	±8	71	±7	65	±4	627	±3
C1-CS	125	±4	77	±2	118	±15	142	±7	58	±11	62	±7	650	±14
C1G0	109	±3	43	±15	104	±5	102	±5	61	±7	56	±2	637	±8
C1-G1	105	±3	94	±2	132	±5	110	±6	67	±3	58	±4	659	±9
C2–S	107	±4	59	±2	96	±10	210	±12	107	±7	98	±4	624	±8
C2-CS	121	±5	55	±2	99	±6	1192	±67	100	±8	95	±4	646	±9
C2-G0	95	±4	50	±3	ND		214	±11	92	±4	93	±4	580	±8
C2-G1	87	±5	59	±2	ND		159	±10	112	±8	105	±4	575	±8

* ND = Not determined.

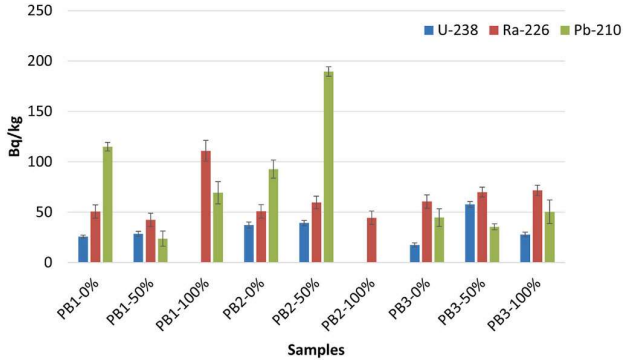

Fig. 5. Values of activity concentration and uncertainties (whiskers) for the elements of U series in the proof bodies (PB) samples made with 0%, 50%, and 100% of niobium waste aggregate material.

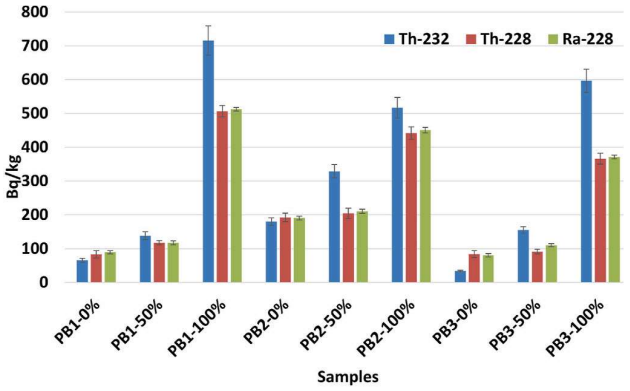

Fig. 6. Activity concentration and uncertainties (whiskers) for the elements of the Th series in the proof bodies (PB) samples made with 0%, 50%, and 100% of niobium waste aggregate material.

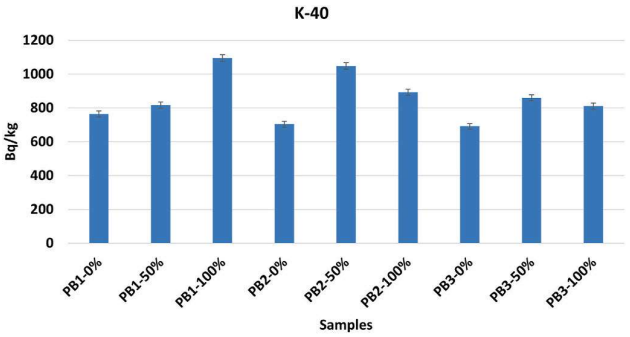

Fig. 7. Activity concentration and uncertainties (whiskers) for ^{40}K in the proof bodies (PB) samples made with 0%, 50%, and 100% of niobium waste aggregate material.

sample PB2-100% was also below the detection limit for ^{210}Pb. The variation observed for the nuclides activity concentration from the ^{238}U series can be due to the significant variation of lithologies found in the mining place resulting in considerable variations of the activity concentrations of the gravel used to make these proof bodies.

Fig. 6 shows the activity concentrations for the Th series. In this case, the general pattern is an increase in activity concentration of ^{232}Th, ^{228}Th, and ^{228}Ra with increasing concentrations of niobium waste employed in the manufacture of the concrete proof bodies. Therefore, as expected, the highest activity concentrations were found in the proof body concretes made using 100% of the niobium aggregate. The activity concentrations measured in the proof bodies concrete, PB1 and PB3, produced with 100% of the niobium aggregate, however, showed much higher values compared to the ones produced with 0 and 50% of aggregates. This difference may be related to the high heterogeneity among the aggregate lithologies (El Hajj et al., 2019) and from the fact that three different batches were used in the proof bodies making. Overall, the activity concentrations of ^{232}Th in PB-100% were reduced in PB-50% from values varying from 500 to 700 Bq kg^{-1} to values varying from 140 to 330 Bq kg^{-1}.

Fig. 7 shows the activity concentrations for the ^{40}K. Here too, a different patter was observed, as the relatively high values were the 50% specimens in both PB-2 and PB-3 series, while the highest value were obtained for 100% specimen in the PB-1 samples. In all cases the values varied in the 700–1100 Bq kg^{-1} range, which is here considered a small variation.

Comparing Figs. 6 and 7 results with the activity concentration index established by the European Commission [38] of 300 Bq kg^{-1}, 200 Bq kg^{-1} and 3000 Bq kg^{-1} for ^{226}Ra, ^{232}Th and ^{40}K, respectively, it is possible to affirm that the addition of up to 50% of aggregates from the niobium industry in the concrete limits the dose to values lower than 1 mSv y^{-1}.

According to the Brazilian Technical Standard 6118 (ABNT 6118, 2003) [39], concrete generally consists of 12–16% appropriate cement and 84–88% of appropriate coarse and fine aggregates, both figures by weight. The aggregates can be mined from either hard rock sources, then crushed, or from sands and gravels [40]. Using recycled material from mining operations certainly contribute to reducing both waste and tailing disposal, as well as reducing the demand for mining material for cement and the concrete industry itself, provided the radiological safety is ensured.

4.1. Radon and thoron exhalation rates

Fig. 8 presents the results for radon and thoron exhalation rates (ER) for the aggregates. The aggregate samples from Industry A, as classified in the sample description sectionlabeled in Fig. 8 S-A (sand), CS-A (crushed stone), G0-A (gravel 0) and G1-A (gravel 1) showed a higher exhalation rate than the aggregates selected in the region (labeled "G" and "PB"), for both ^{222}Rn and ^{220}Rn. "S" stands for sand, "CS" stands for crushed stone, "G0" stands for gravel 0, and "G1" stands for gravel 1. Accordingly, the ER for thoron was four orders of magnitude higher than those of radon, as it is usually found for different materials applied for construction shown in Table 2. For thoron, the values reported may be underestimated as the nuclide transfer time to the Rad7 was not considered. Moreover, the use of a closed-circuit may also bring more inaccuracy into the thoron measurements.

The ER obtained for the plate samples, as presented in Fig. 9, showed that plates prepared with cement type CPII (P1, P2, P3) resulted in higher ^{222}Rn and ^{220}Rn exhalation rates than plates prepared with cement CPV-ARI type (P4, P5, P6). The cement CPII is meant for general use and the final concrete tends to present high permeability. In contrast, the cement CPV-ARI is a high resistance cement that tends to manufacture low permeability concrete. This may indicate that the latter cement provides a less porous concrete structure, therefore reducing the radon and thoron scape.

Fig. 10 shows the results obtained for the radon and thoron ER of the proof bodies. All proof bodies samples were manufactured with the cement CPII (for general use) and niobium waste in different concentrations. The result for sample PB1-50% could not be determined for radon, and a high value with high uncertainty was observed for sample PB2-0%, probably due to the very low ^{222}Rn ER, although all samples have been measured in the same conditions. Radon ER was much lower than that observed for thoron, and no clear correlation could be observed between the ER values and the amount of residue used in the proof body preparation. One possibility that should be investigated is the bulk density and total pore volume of each proof body according to their residue composition. The variability in niobium waste activity concentration should be further investigated using a variogram as the activity concentration seem to vary significantly from batch to batch.

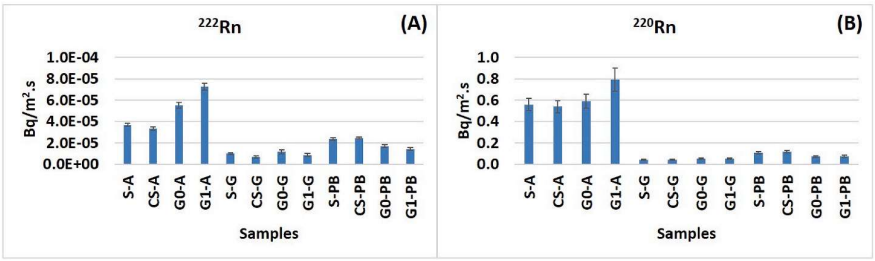

Fig. 8. Exhalation rates of ^{222}Rn (A) and ^{220}Rn (B), and uncertainties (whiskers), in the aggregate samples.

Table 2
Exhalation rate (ER in Bq m^{-2} s^{-1}) for radon and thoron found in different construction materials based on [41–45].

	^{222}Rn range	^{220}Rn range	Refer
Granite	0.06 ± 0.01	76 ± 34	[37]
	1.04 ± 0.03	2420 ± 667	
Granite	0.7	2515	[38]
	1.33	5900	
Cement	0.00049 ± 0.00001		
Aerated concrete		75	[39]
Concrete		96	
Concrete	0.4 ± 0.1		[40]
Sand	0.00029 ± 0.00002		[41]
Sand	0.008 ± 0.002		[40]
Aggregate	0.00150 ± 0.00006		[40]
Aggregate	0.00044 ± 0.00003		[41]
Brick	3.09	100	[38]
Brick	7.07	640	[38]

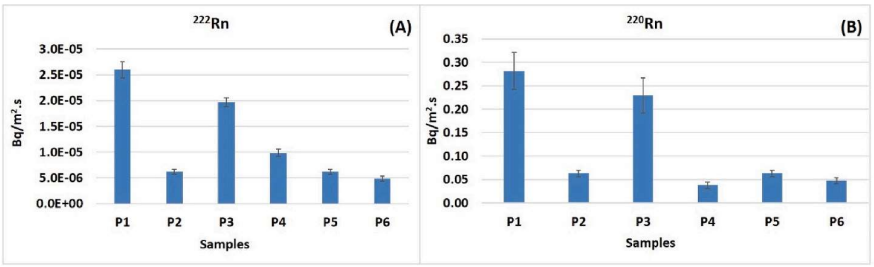

Fig. 9. Exhalation rate of ^{222}Rn (A) and ^{220}Rn (B), and uncertainties (whiskers), in the plate samples made with the niobium aggregate.

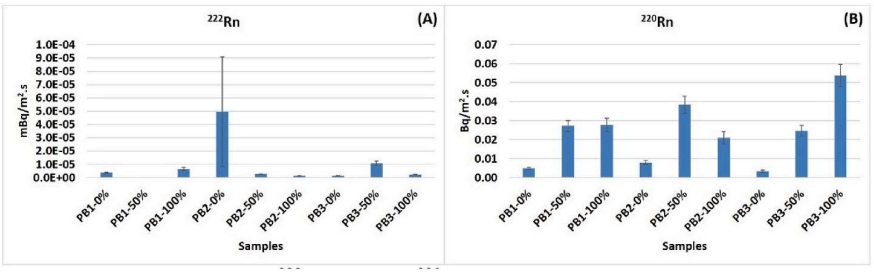

Fig. 10. Exhalation rate of ^{222}Rn (A) and ^{220}Rn (B) and uncertainties (whiskers), in the proof bodies samples.

5. Conclusions

This study evaluated the activity concentration of U and Th series nuclides and ^{40}K, and ^{222}Rn and ^{220}Rn exhalation rates for niobium waste with physical properties suitable to be used as aggregates (sand, crushed stones, gravel 0 and gravel 1), and concrete

plates and proof bodies produced using niobium waste. The goal was to test the feasibility of using niobium waste as construction material. Moreover, we analyzed common commercially available aggregates and cement for comparison.

The activity concentrations of Th series nuclides are much higher in Industry A aggregated samples than observed for the same type of material obtained in the local market. Also, the non-classified waste sample analyzed here presented higher Th nuclides series activity concentration than the classified aggregates, however, it is not clear if resulting from the heterogeneity of the samples or from the wet sieving employed. These high activities justify the need for thoron measurements in the aggregates, despite its low half-life. The use of the analyzed niobium aggregates in the proportion of 50% of the concrete aggregates may reduce the total activity concentrations of the final product. The exhalation rates for ^{222}Rn and ^{220}Rn in the plates and proof body produced with the aggregates resulting from the niobium mining operations are in the same range of common materials regularly employed in construction. Moreover, the use of cement of CPV-ARI type resulted in concrete with a lower exhalation rate. The high activities encountered in these materials may threaten human health if used for dwellings due to the gamma exposition. Nevertheless, to reduce the amount of waste generated in the mining industry, the Industry A aggregate may be applied for the construction of outdoor structures such as bridges, viaducts, and roadbeds where exhaled radon cannot be accumulated and public individuals do not spend a considerable amount of time.

Regarding the limitations and recommendations for future works, it is crucial to consider the impacts the radioactivity may have on the physical integrity of the concrete on a long-term basis.

CRediT author statement

Paulo Sergio Cardoso da Silva: Formal analysis, Methodology, Writing - original draft, review, and editing. **Thammiris Mohamad El Hajj**: Conceptualization, Methodology, Writing - review and editing. **Gabriel A. S. A. Dantas**: Methodology, Formal analysis. **Homero Delboni Jr.**: Data curation. **Mauro Gandolla**: Conceptualization, Methodology.

Declaration of competing interest

The authors declare that they have no known competing financial interests or personal relationships that could have appeared to influence the work reported in this paper.

References

[1] R. El Zrelli, L. Rabaoui, P. van Beek, S. Castet, M. Souhaut, M. Grégoire, P. Courjault-Radé, Natural radioactivity and radiation hazard assessment of industrial wastes from the coastal phosphate treatment plants of Gabes (Tunisia, Southern Mediterranean Sea), Mar. Pollut. Bull. 146 (2019) 454–461.
[2] M.M. Hamed, M.A. Hilal, E.H. Borai, Chemical distribution of hazardous natural radionuclides during monazite mineral processing, J. Environ. Radioact. 162 (163) (2016) 166–171.
[3] A. Goronovski, R.M. Rivera, T. Van Gerven, A.H. Tkaczyk, Radiological assessment of bauxite residue processing to enable zero-waste valorisation and regulatory compliance, J. Clean. Prod. 294 (2021) 125165.
[4] J.A. Galhardi, R. García-Tenorio, D.M. Bonotto, I. Díaz-Francés, J.G. Motta, Natural radionuclides in plants, soils and sediments affected by U-rich coal mining activities in Brazil, J. Environ. Radioact. 177 (2017) 37–47.
[5] Y.J. Huang, C.F. Chen, Y.C. Huang, Q.J. Yue, C.M. Zhong, C.J. Tan, Natural radioactivity and radiological hazards assessment of bone-coal from a vanadium mine in central China, Radiat. Phys. Chem. 107 (2015) 82–88.
[6] T.M. El Hajj, M.P.A. Gandolla, P.S.C. da Silva, H. Torquato, H. Delboni, Long-term prediction of non-processed waste radioactivity of a niobium mine in Brazil, J. Sustain. Min. 18 (3) (2019) 142–149.
[7] P.P. Haridasan, Managing exposure to natural sources: International standards and new challenges, in: Proceedings of the Seventh International Symposium on Naturally Occurring Radioactive Material (NORM VII). Beijing, China, 2013, 978–92–0–104014–5, 22-26 April 2013. p. 24 cm. — (Proceedings series, ISSN 0074–1884) STI/PUB/1664.
[8] Naturally Occurring Radioactive Material, IAEA - International Atomic Energy Agency, 2019. https://www.iaea.org/topics/radiation-safety-norm. (Accessed 27 July 2019). Accessed.
[9] Gael Bellenfant, Anne-Gwénaëlle Guezennec, Francoise Bodenan, Patrick d'Hugues, Daniel Cassard, Re-processing of Mining Waste: Combining Environmental Management and Metal Recovery? Mine Closure Conference, Sep, Cornwall, United Kingdom, 2013, pp. 571–582, https://doi.org/10.36487/ACG_rep/1352_48_Bellenfant.
[10] M. Tayebi-Khorami, M. Edraki, G. Corder, A. Golev, Re-thinking mining waste through an integrative approach led by circular economy aspirations, Minerals 286 (9) (2019) 1–12.
[11] H. Liu, Z. Pan, NORM situation in non-uranium mining in China, Ann. ICRP 41 (3–4) (2012) 343–351.
[12] H.A. van der Sloot, D.S. Kosson, N. Impens, N. Vanhoudt, T. Almahayni, H. Vandenhove, L. Sweeck, R. Wiegers, J.L. Provis, C. Gascó, W. Schroeyers, Leaching assessment as a component of environmental safety and durability analyses for NORM containing building materials, in: Wouter Schroeyers, Naturally Occurring Radioactive Materials in Construction, Woodhead Publishing, 2017, pp. 253–288, https://doi.org/10.1016/b978-0-08-102009-8.00008-6.
[13] B. Michalik, G. de With, W. Schroeyers, Measurement of radioactivity in building materials – problems encountered caused by possible disequilibrium in natural decay series, Construct. Build. Mater. 168 (2018) 995–1002.
[14] D. Nizevičienė, D. Vaičiukynienė, B. Michalik, M. Bonczyk, V. Vaitkevičius, V. Jusas, The treatment of phosphogypsum with zeolite to use it in binding material, Construct. Build. Mater. 180 (2018) 134–142.
[15] Z. Sas, N. Vandevenne, R. Doherty, R. Vinai, J. Kwasny, M. Russell, W. Sha, M. Soutsos, W. Schroeyers, Radiological evaluation of industrial residues for construction purposes correlated with their chemical properties, Sci. Total Environ. 658 (2019) 141–151.
[16] S. Donatello, C.R. Cheeseman, Recycling and recovery routes for incinerated sewage sludge ash (ISSA): a review, Waste Manag. 33 (2013) 2328–2340.
[17] A. Wongsa, K. Boonserm, C. Waisurasingha, V. Sata, P. Chindaprasirt, Use of municipal solid waste incinerator (MSWI) bottom ash in high calcium fly ash geopolymer matrix, J. Clean. Prod. 148 (2017) 49–59.
[18] A. Goronovski, P.J. Joyce, A. Björklund, G. Finnveden, A.H. Tkaczyk, Impact assessment of enhanced exposure from naturally occurring radioactive materials (NORM) within LCA, J. Clean. Prod. 172 (2018) 2824–2839.
[19] K. Kovler, H. Friedmann, B. Michalik, W. Schroeyers, A. Tsapalov, S. Antropov, T. Bituh, D. Nicolaides, Basic aspects of natural radioactivity, Nat. Occurring Radioact. Mater. Construct. (2017), https://doi.org/10.1016/B978-0-08-102009-8.00003-7.
[20] M. Hosoda, H. Kudo, K. Iwaoka, R. Yamada, T. Suzuki, Y. Tamakuma, S. Tokonami, Characteristic of thoron (220Rn) in environment, Appl. Radiat. Isot. 120 (2017) 7–10.

[21] G.S. Bineng, Saïdou, S. Tokonami, M. Hosoda, Y.F.T. Siaka, H. Issa, T. Suzuki, H. Kudo, O. Bouba, The importance of direct progeny measurements for correct estimation of effective dose due to radon and thoron, Front. Public Health 8 (2020) 1–17.
[22] IAEA. International Atomic energy agency, Radiation Protection and Safety of Radiation Sources: International Basic Safety Standards (BSS), GSR Part 3, International Atomic Energy Agency, Vienna, Austria, 2014.
[23] Maria Karpińska, Zenon Mnich, Jacek Kapała, Seasonal changes in radon concentrations in buildings in the region of northeastern Poland, J. Environ. Radioact. 77 (2004) 101e109, https://doi.org/10.1016/j.jenvrad.2004.02.005.
[24] J.C. Scholten, I. Osvath, M.K. Pham, ^{226}Ra measurements through gamma spectrometric counting of radon progenies: how significant is the loss of radon? Mar. Chem. 156 (2013) 146–152.
[25] N.H. Cutshall, L.H. Larsen, C.R. Olsen, Direct analysis of ^{210}Pb in sediment samples: self-absorption corrections, Nucl. Instrum. Methods Phys. Res. 206 (1–2) (1983) 1983.
[26] R.R. Greenberg, P. Bode, E.A. De Nadai Fernandes, Neutron activation analysis: a primary method of measurement, Spectrochim. Acta B Atom Spectrosc. 66 (3–4) (2011) 193–241.
[27] RAD7 Radon detector, User Manual, Durridge Company Inc, http://www.durridge.com/documentation/RAD7 Manual.pdf, 27 Ago 2019.
[28] P. Tuccimei, M. Moroni, D. Norcia, Simultaneous determination of ^{222}Rn and ^{220}Rn exhalation rates from building materials used in Central Italy with accumulation chambers and a continuous solid state alpha detector: influence of particle size, humidity, and precursors concentration, Appl. Radiat. Isot. 64 (2) (2006) 254–263.
[29] S. de Martino, C. Sabbarese, G. Monetti, Radon emanation and exhalation rates from soils measured with an electrostatic collector, Appl. Radiat. Isot. 49 (4) (1998) 407–413.
[30] T.M. El Hajj, M.P.A. Gandolla, P.S.C. Silva, E.L. Juliao, J.L.G. Villanueva, H. Delboni JR., A method for radiologically evaluating indoor use of dimension stone considering radon exhalation rates, J. Eur. Radon Assoc. 1 (2020) 1–15.
[31] R.H. Worden, D.A.C. Manning, P.R. Lythgoe, The origin and production geochemistry of radioactive lead (210Pb) in NORM-contaminated formation waters, J. Geochem. Explor. 69 (70) (2000) 695–699.
[32] A. Eštoková, L. Palaščáková, Assessment of natural radioactivity levels of cements and cement composites in the Slovak republic, Int. J. Environ. Res. Publ. Health 10 (2013) 7165–7179.
[33] BE Özdiş, N.F. Çam, B. Canbaz Öztürk, Assessment of natural radioactivity in cements used as building materials in Turkey, J. Radioanal. Nucl. Chem. 311 (2018) 307–316.
[34] R.G. Reis, NORM: Guia Prático, Rócio Glória dos Reis, Rio de Janeiro, 2016.
[35] Turhan Ş, Assessment of the natural radioactivity and radiological hazards in Turkish cement and its raw materials, J. Environ. Radioact. 99 (2) (2008) 404–414.
[36] T.M. El Hajj, M.P.A. Gandolla, P.S.C. Silva, H. Torquato, H. Delboni Junior, Long-term prediction of non-processed waste radioactivity of a niobium mine in Brazil, J. Sustain. Min. 18 (2019) 142–149.
[37] J.L. Antoniassi, D. Uliana, R. Contessotto, H. Kahn, C. Ulsen, Process mineralogy of rare earths from deeply weathered alkali-carbonatite deposits in Brazil, J. Mater. Res. Technol. 9 (4) (2020) 8842–8853.
[38] European Commission, Radiation Protection 112 Radiological Protection Principles Concerning the Natural Radioactivity of Building Materials, European Union, Luxembourg, 1999. http://ec.europa.eu/energy/nuclear/radiation protection/doc/publication/112.pdf.
[39] ABNT, Projeto de estruturas de concreto – procedimento. Associação Brasileira de Normas Técnicas, 2003. ABNT NBR 6118.
[40] N. Tangtinthai, O. Heidrich, D.A.C. Manning, Role of policy in managing mined resources for construction in Europe and emerging economies, J. Environ. Manag. 236 (2019) 613–621.
[41] N.M. Hassan, T. Ishikawa, M. Hosoda, K. Iwaoka, A. Sorimachi, S.K. Sahoo, M. Janik, C. Kranrod, H. Yonehara, M. Fukushi, S. Tokonami, The effect of water content on the radon emanation coefficient for some building materials used in Japan, Radiat. Meas. 46 (2) (2011) 232–237.
[42] M. Janik, Y. Omori, H. Yonehara, Influence of humidity on radon and thoron exhalation rates from building materials, Appl. Radiat. Isot. 95 (2015) 102–107.
[43] G. de With, R.C.G.M. Smetsers, H. Slaper, P. de Jong, Thoron exposure in Dutch dwellings – an overview, J. Environ. Radioact. 183 (2018) 73–81.
[44] A. Kumar, R.P. Chauhan, M. Joshi, B.K. Sahoo, Modeling of indoor radon concentration from radon exhalation rates of building materials and validation through measurements, J. Environ. Radioact. 127 (2014) 50–55.
[45] R.G. Sonkawade, K. Kant, S. Muralithar, R. Kumar, R.C. Ramola, Natural radioactivity in common building construction and radiation shielding materials, Atmos. Environ. 42 (9) (2008) 2254–2259.